Unbiased White Matter Atlas Construction Using Diffusion Tensor Images

Hui Zhang[1], Paul A. Yushkevich[1], Daniel Rueckert[2], and James C. Gee[1]

[1] Penn Image Computing and Science Laboratory (PICSL), Department of Radiology, University of Pennsylvania, Philadelphia, USA
[2] Department of Computing, Imperial College, London, UK

Abstract. This paper describes an algorithm for unbiased construction of white matter (WM) atlases using full information available to diffusion tensor (DT) images. The key component of the proposed algorithm is a novel DT image registration method that leverages metrics comparing tensors as a whole and optimizes tensor orientation explicitly. The problem of unbiased atlas construction is formulated using the approach proposed by Joshi et al., i.e., the unbiased WM atlas is determined by finding the mappings that best match the atlas to the images in the population and have the least amount of deformation. We show how the proposed registration algorithm can be adapted to approximately find the optimal atlas. The utility of the proposed approach is demonstrated by constructing a WM atlas of 13 subjects. The presented DT registration method is also compared to the approach of matching DT images by aligning their fractional anisotropy images using large-deformation image registration methods. Our results suggest that using full tensor information can better align the orientations of WM fiber bundles.

1 Introduction

Diffusion tensor imaging (DTI) is a unique imaging technique that probes microscopic tissue properties by measuring local diffusion of water molecules [3]. Its demonstrated ability to depict *in vivo* the intricate architecture of white matter (WM) [4] has made it an invaluable tool for furthering our understanding of WM both in normal populations and in populations with brain disorders. Wakana et al. [5] provided a powerful illustration of this new insight into WM by building an annotated WM atlas delineated via semi-automatic tractography-based segmentation on a single-subject anatomy.

From the perspective of computational neuroanatomy, DTI also offers an exciting opportunity for the construction of an unbiased WM atlas, i.e., a standard coordinate system not biased by the anatomy of a particular subject but representing the complex variability within the whole population of interest. Such atlas can serve as a deformable template, which will enable detailed atlas information to be mapped to individual subject spaces [6]. Another important application of such atlas is in identifying as well as localizing WM differences across populations using DTI. In this scenario, individual images are mapped

N. Ayache, S. Ourselin, A. Maeder (Eds.): MICCAI 2007, Part II, LNCS 4792, pp. 211–218, 2007.

to the stereotactic space defined by the atlas, thereby removing shape differences among the individuals. On one hand, any change in microstructural tissue properties of shared anatomies, e.g., the mean rate of diffusion or the diffusion anisotropy, can be examined. On the other hand, the shape differences or variabilities encoded in the transformations that define the mapping between individual to the atlas are essential for the understanding of volumetric changes in WM structures.

The key element in the construction of such a WM atlas is an effective image registration algorithm that establishes accurate mapping of common WM structures between images. Goodlett et al. [7] demonstrated the advantage of using large-deformation registration over affine registration for this purpose. The authors aligned WM structures by registering the scalar images derived from the fractional anisotropy (FA) images that were in turn derived from DT images. In this paper we describe the construction of such a WM atlas using a novel DT registration algorithm. Compared to [7], the registration algorithm proposed here takes full advantage of the relevant information encoded in DT images, particularly the tensor orientation, thus enabling more faithful alignment of different WM tracts, as first demonstrated in [8].

The rest of the paper is organized as follows. Sec. 2 describes the proposed DT registration algorithm while Sec. 3 gives details of its application to WM atlas construction. In Sec. 4, the preliminary results of applying the proposed procedure to a large database are presented and we report the quantitative analysis of the behavior and the performance of the proposed DT registration algorithm. A comparison of aligning DT images using the proposed registration algorithm to the approach of aligning their FA images using large-deformation registration methods suggest that using full tensor information can better align the orientations of WM fiber bundles. Future directions are discussed in Sec. 5.

2 Diffusion Tensor Image Registration

The DT image registration algorithm proposed here is an extension of the deformable DT image registration method that we recently proposed in [1]. The algorithm described in [1] models transformations as piecewise affine and leverages full tensor-based similarity metrics while optimizing tensor orientation explicitly. In addition, the derivatives of the registration cost function are analytic, enabling both fast and accurate derivative-based optimization. However, the algorithm, by design, is most accurate when deformation is not large, thus can render less optimal results when deformation becomes large. The extension proposed here aims to address this limitation of the algorithm without forgoing its advantages. Below we first summarize the algorithm in [1] and then describe our specific enhancements.

2.1 Piecewise Affine Algorithm

The algorithm in [1] approximates smooth transformations using a dense piecewise affine parametrization which is sufficient when the required deformations are not large. The dense piecewise affine parametrization effectively divides the template space into uniform regions and parametrizes the transformation within each region by an affine transformation. The registration cost function consists of an image matching term (the likelihood) and a transformation smoothness term (the prior). The image term is the summation of the region-wise tensor image difference determined via a particular choice of tensor metric $\|.\|$. For a particular region Ω, the linear part of the associated affine transformation is parametrized using the matrix polar decomposition, such that $\mathbf{x} \mapsto (QS)\mathbf{x} + \mathbf{T}$, where Q is a special orthogonal matrix representing the pure rotation, S is a symmetric positive definite matrix representing the pure deformation and $\mathbf{T}$ is the translation vector. By using the finite strain tensor reorientation [9], the image term is formulated as

$$\phi(\mathbf{p}) = \int_{\Omega} \|\mathbf{I}_s((QS)\mathbf{x} + \mathbf{T}) - Q\mathbf{I}_t(\mathbf{x})Q^{\mathrm{T}}\|^2 \, d\mathbf{x} \ , \tag{1}$$

where $\mathbf{I}_t$ and $\mathbf{I}_s$ are the template (fixed) and subject (moving) DT images respectively, and $\mathbf{p}$ denotes the 12 affine parameters. The overal smoothness of the piecewise affine transformation is regularized by penalizing the discontinuities across region boundaries. For two adjacent regions Ω_i and Ω_j with the associated affine transformations being F_i and F_j respectively, the discontinuity is formulated as

$$\int_{\Omega_i \cap \Omega_j} \|F_i(x) - F_j(x)\| dx, \tag{2}$$

where $\|.\|$ denotes the vector norm. The dense piecewise affine approximation to the underlying transformation is estimated and refined in a hierarchical framework by beginning with coarse subdivision of template space then continuing with finer subdivision. The transformation estimated at the finest level is interpolated using the standard approach [10] to generate a smooth warp field which is then used to deform the subject into the space of the template with the PPD reorientation strategy [9].

Although the algorithm is applicable for general tensor similarity measures, we chose to use the tensor metric that measures the L^2 distance between the anisotropic part of the apparent diffusion profiles associated with the DTs that we first described in [1]. Under this metric, the distance between two DTs $\mathbf{D}_1$ and $\mathbf{D}_2$ is equal to

$$\sqrt{\frac{8\pi}{15}(\|\mathbf{D}_1 - \mathbf{D}_2\|_C^2 - \frac{1}{3}\mathrm{Tr}^2(\mathbf{D}_1 - \mathbf{D}_2))} \ , \tag{3}$$

where $\|\mathbf{D}_1 - \mathbf{D}_2\|_C$ is the Euclidean distance between the two tensors and equal to $\sqrt{\mathrm{Tr}((\mathbf{D}_1 - \mathbf{D}_2)^2)}$. This choice is consistent with the seminal observations by Pierpaoli et al in [4] that in human brain the isotropic part of diffusion are similar in values in grey and white matter regions. Hence, a metric focusing on identifying differences in anisotropic diffusion can be more optimal by ignoring differences in isotropic diffusion that are likely a result of noise or partial volume contamination in the data.

2.2 Enhancements to the Piecewise Affine Algorithm

The proposed extension handles larger deformations by both enhancing the piecewise affine algorithm itself and by iteratively composing smaller incremental deformations estimated using the enhanced piecewise affine algorithm.

The enhancement to the piecewise affine algorithm aims to ensure that resulting deformation fields have physically meaningful Jacobian (matrix) determinant values, i.e., being positive and not close to be singular. The affine parametrization proposed in [1] parametrizes the pure deformation S using its six linearly independent components. This parametrization does not forbid S to have negative determinant and this undesirable scenario did occur in practice in our experimentation. We propose to instead parametrize the pure deformation S using its Cholesky decomposition, i.e., $S = LL^{\mathrm{T}}$, where L is a lower triangular matrix. In this scheme, S is now parametrized by the six non-zero elements in L and is guaranteed to be positive semidefinite. To penalize Jacobian determinant close to be singular, we add a Jacobian prior term adopted from [11], which is

$$\mathrm{T}r(S^2 + S^{-2} - 2\mathbf{I}) = \sum_{i=1}^{3}(s_i^2 + s_i^{-2} - 2), \tag{4}$$

where s_i are the ith eigenvalues of S. Observe that this prior term is zero when S is the identity matrix and increases when any of the eigenvalues s_i deviates from 1.

Our second strategy for better handling large deformations is to use the enhanced piecewise affine algorithm to incrementally estimate the underlying true deformation. Given N successively determined incremental deformations $\{P_i\}_{i=1}^{N}$, the final deformation is determined by their compositions, i.e., $\mathbf{x} \mapsto P_1 \circ P_2 \circ ... \circ P_i \circ ... \circ P_{N-1} \circ P_N(\mathbf{x})$. During each incremental estimation, we set the weightings of both prior terms to stringent values such that large deformation is penalized and the incremental dense piecewise affine transformation is sufficiently close to the corresponding interpolated smooth deformation. The sufficient values for these weights can be empirically determined for a particular dataset. However, given that the DTs take physical values and overall don't differ significantly across different datasets, we have found in practice that these weights, once determined for one dataset, worked well for others. The weightings that we have found worked well in practice are 0.08 for the smoothness prior and 0.2 for the Jacobian prior. The number of incremental estimation steps that we found sufficient is between 5 and 6. Each incremental estimate takes about 10 mins or less on a modern 3.0GHz Intel Xeon processor and the total estimation usually takes less than one hour.

3 Unbiased White Matter Atlas Construction

We formulate the unbiased atlas construction problem according to the approach proposed by Joshi et al. in [2]. Joshi et al. stated the unbiased atlas construction problem as estimating an image that requires the minimum amount of deformation to map into every image in the population. In our context, given a population of N DT images $\{\mathbf{I}_i\}_{i=1}^N$, the atlas estimation problem can then be defined as

$$\{\hat{H}_i, \hat{\mathbf{I}}\} = \arg\min_{H_i,\mathbf{I}} \sum_{i=1}^{N} (\int_{\mathbb{R}^3} \|\mathbf{I}_i \circ H_i(\mathbf{x}) - \mathbf{I}(\mathbf{x})\|^2 d\mathbf{x} + D(H_i)), \tag{5}$$

where H_i is the deformation applied to the image $\mathbf{I}_i$ and $D(H_i)$ is some appropriate metric quantifying the amount of deformation associated with H_i.

It can be shown that under the tensor metric Eqn. 3, the image that minimizes Eqn. 5, when the transformations $\{H_i\}_{i=1}^N$ are fixed, is simply

$$\hat{\mathbf{I}}(\mathbf{x}) = \frac{1}{N} \sum_{i=1}^{N} \mathbf{I}_i \circ H_i(\mathbf{x}). \tag{6}$$

This result is completely analogous to the result in [2] for the sum of squared error scalar image similarity metric, which allows us to use an algorithm similar to the iterative greedy method used to minimize Eqn. 5 in [2].

Our iterative algorithm is as follows. At iteration $m, m \geq 0$, the atlas estimate $\hat{\mathbf{I}}^{(m)}$ is estimated using Eqn. 6 with $H_i = H_i^{(m)} = P_i^{(0)} \circ P_i^{(1)} \circ ...P_i^{(m)}(\mathbf{x})$ where $P_i^{(m)}$ is the estimated incremental dense piecewise affine transformation for the ith image at iteration m. When $m = 0$, $\{P_i^{(0)}\}_{i=1}^N$ are initialized to the identity transformation and the initial atlas $\hat{\mathbf{I}}^{(0)}$ is computed as an average of the original subject DT images $\{\mathbf{I}_i\}_{i=1}^N$. When $m \geq 1$, $\{P_i^{(m)}\}_{i=1}^N$ are estimated by registering the DT images $\{\mathbf{I}_i \circ H_i^{(m-1)}\}_{i=1}^N$ to the atlas estimate $\hat{\mathbf{I}}^{(m-1)}$ using the piecewise affine algorithm described in Sec. 2. In this implementation, the amount of deformation $D(H_i)$ is approximated via the two prior terms discussed in Sec. 2. For our current implementation, we have found that the sufficient number of incremental iterations N for the estimated atlas to converge is around 6. The convergence is checked by estimating $\|\hat{\mathbf{I}}^{(m)} - \hat{\mathbf{I}}^{(m-1)}\|$. In practice, this procedure is applied to the subject images after they have been corrected for global size and pose differences using affine registration.

4 Experiments and Results

We demonstrate the performance of the proposed algorithm by applying it to construct a WM atlas from 13 DT images drawn from a large MR imaging database. MRI was performed on a Philips 3-Tesla system with maximum gradient strength of 62 mT/m on each independent axis and slew rate of 100 mT/m/ms on each axis using a 6-channel phased array head coil. Diffusion-weighted images were acquired with a single-shot echo-planar diffusion-weighted sequence with 15 non-collinear gradient directions @ b = 1000 s/mm^2 with a SENSE factor of 2. The additional imaging parameters are as follows: TR 12000ms, TE 51ms, slice thickness 2mm, field of view 224mm, matrix 128 x 128, resulting in voxel size 1.75 x 1.75 x 2 mm^3.

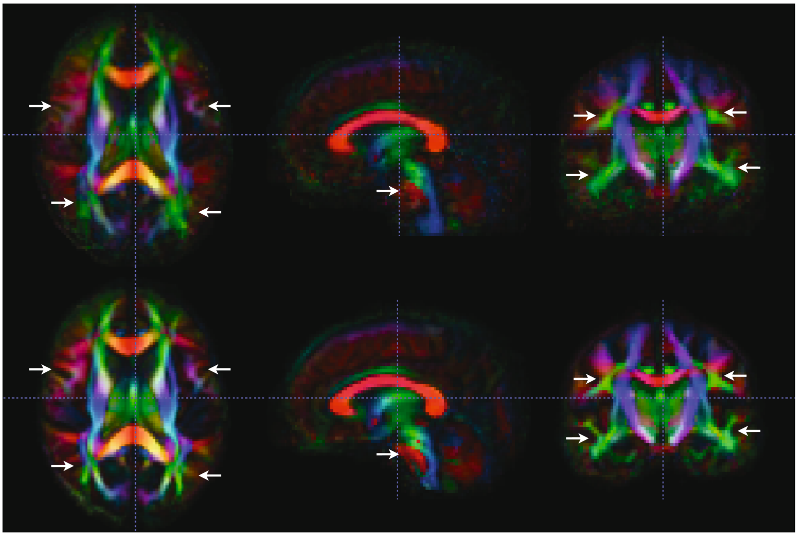

Fig. 1. Comparison of the atlas constructed from affine registered images (top row) to the atlas constructed from registered images using the proposed algorithm (bottom row). The regions with more prounounced differences are highlighted with arrows. The RGB image encodes the principal diffusion directionss: red for left-right, green for anterior-posterior and blue for inferior-superior [12].

We applied the proposed algorithm to the DT images reconstructed from the diffusion-weighted images using the standard linear regression [3]. The atlas constructed is shown in fig. 1 along with the initial atlas constructed from affinely aligned images. Compared to the initial atlas (top row), the final atlas (bottom row) has considerably sharper edge features as well as much richer details in the cortical regions.

To demonstrate the behavior and the performance of the enhanced piecewise affine registration algorithm, the algorithm is used to register the affine registered images to the constructed unbiased atlas with 6 incremental steps. We quantitatively assessed the overall quality of spatial normalization after each incremental step using two voxelwise statistics: *normalized FA standard deviation* $\bar{\sigma}_{FA}$ and *dyadic coherence* κ. Since diffusion anisotropy and the dominant direction of diffusion are two features that account for most of the variations in WM [4], misalignment that renders different WM structures being mapped to one another should yield large voxelwise variations in either one or both of the features. The two voxelwise statistics directly assess these variations and hence can be indicative of misalignment of WM structures. Given a set of DTs sampled at some voxel from the normalized images after a particular incremental step, $\bar{\sigma}_{FA}$ is defined as the ratio of the standard deviation and mean of the FA values of these DTs, and κ [13] takes values that range from 0 to 1 (0 for randomly oriented directions and 1 for identically oriented directions). These statistics were computed for the voxels with FA > 0.2 in the atlas. The resulting statistical maps from different incremental steps were compared using their respective empirical cumulative distribution functions (CDF). The method producing better spatial alignment should result in more reduction in $\bar{\sigma}_{FA}$ and larger increase in κ, which in turn will be reflected as its $\bar{\sigma}_{FA}$ and κ CDFs being more to the left and to the right, respectively. The performance of the algorithm is compared against both the initial affine alignment and the alignment rendered using a large-deformation scalar registration method which optimizes a cross-correlation metric under the constraints of a diffeomorphic transformation model in multi-resolution and symmetric fashion [14]. The large-deformation algorithm is applied to normalize the FA images of the affine-aligned DT images to the FA image of the unbiased DT atlas. The results are shown in Fig. 2. It shows that, by taking incremental steps, the proposed algorithm is able to gradually improve the quality of normalization with respect to both $\bar{\sigma}_{FA}$ and κ. With respect to $\bar{\sigma}_{FA}$, the proposed algorithm can perform almost on par with the large-deformation algorithm registering FA images. With respect to κ, the proposed algorithm performs substantially better than the large-deformation algorithm, reflecting the benefit of aligning DT images using full tensor metrics.

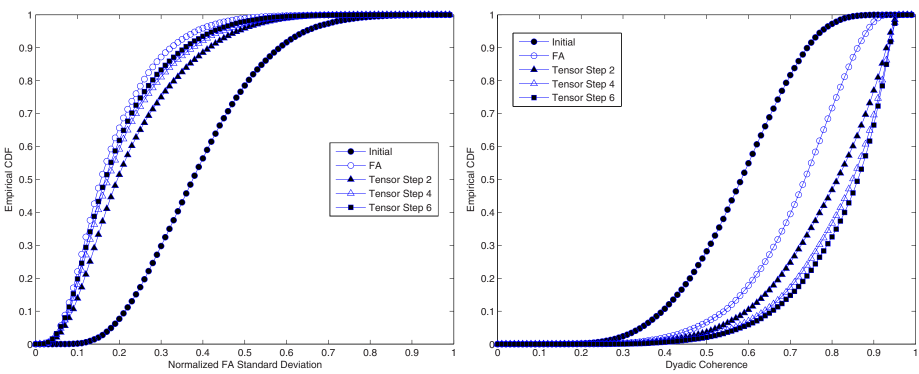

Fig. 2. The empirical CDFs of both $\bar{\sigma}_{FA}$ and κ derived from the initial affine aligned images (Initial), the images aligned using the large-deformation FA registration (FA), and the images aligned using the proposed algorithm at 3 stages (Tensor Step 2, 4 and 6)

5 Discussion

In this paper we have described an algorithm for unbiased WM atlas construction that leverages a novel high-dimensional DT registration algorithm. The strength of the proposed algorithm lies in its ability to optimally align WM structures. The current approach however is limited in its ability to accurately assess the amount of deformation. We plan to address this issue by leveraging the recent work by Arsigny et al. [15], which enables the construction of diffeomorphic maps from piecewise affine transformations. The ability to create diffeomorphic interpolation of the estimated piecewise affine transformations will afford us the principled approach to estimate the amount of deformation in the metric space of diffeomorphisms.

Acknowledgment. The authors gratefully acknowledge support of this work by the NIH via grants EB006266, NS045839, HD046159, HD042974 and MH068066.

References

1. Zhang, H., Yushkevich, P.A., Alexander, D.C., Gee, J.C.: Deformable registration of diffusion tensor MR images with explicit orientation optimization. MIA 10 (2006)
2. Joshi, S., Davis, B., Jomier, M., Gerig, G.: Unbiased diffeomorphic atlas construction for computational anatomy. NeuroImage 23 (2004)
3. Basser, P.J., Mattiello, J., Bihan, D.L.: Estimation of the effective self-diffusion tensor from the NMR spin echo. JMR 103 (1994)
4. Pierpaoli, C., Jezzard, P., Basser, P.J., Barnett, A., Chiro, G.D.: Diffusion tensor MR imaging of the human brain. Radiology 201 (1996)
5. Wakana, S., Jiang, H., Nagae-Poetscher, L.M., van Zijl, P.C., Mori, S.: Fiber tract-based atlas of human white matter anatomy. Radiology 230 (2004)
6. Grenander, U.: General pattern theory. Oxford Univ. Press, Oxford (1994)
7. Goodlett, C., Davis, B., Jean, R., Gilmore, J., Gerig, G.: Improved correspondence for DTI population studies via unbiased atlas building. In: Larsen, R., Nielsen, M., Sporring, J. (eds.) MICCAI 2006. LNCS, vol. 4190, Springer, Heidelberg (2006)
8. Park, H.J., Kubicki, M., Shenton, M.E., Guimond, A., McCarley, R.W., Maier, S.E., Kikinis, R., Jolesz, F.A., Westin, C.F.: Spatial normalization of diffusion tensor MRI using multiple channels. NeuroImage 20 (2003)
9. Alexander, D.C., Pierpaoli, C., Basser, P.J., Gee, J.C.: Spatial transformations of diffusion tensor magnetic resonance images. TMI 20 (2001)
10. Little, J.A., Hill, D.L.G., Hawkes, D.J.: Deformations incorporating rigid structures. CVIU 66 (1997)
11. Ashburner, J., Andersson, J.L.R., Friston, K.J.: Image registration using a symmetric prior — in three dimensions. HBM 9 (2000)
12. Pajevic, S., Pierpaoli, C.: Color schemes to represent the orientation of anisotropic tissues from diffusion tensor data: application to white matter fiber tract mapping in the human brain. MRM 42 (1999)
13. Jones, D.K., Griffin, L.D., Alexander, D.C., Catani, M., Horsfield, M.A., Howard, R., Williams, S.C.R.: Spatial normalization and averaging of diffusion tensor MRI data sets. NeuroImage 17 (2002)
14. Avants, B.B., Gee, J.C.: Geodesic estimation for large deformation anatomical shape averaging and interpolation. NeuroImage 23 (2004)
15. Arsigny, V., Commowick, O., Pennec, X., Ayache, N.: A log-euclidean polyaffine framework for locally rigid or affine registration. In: Pluim, J.P.W., Likar, B., Gerritsen, F.A. (eds.) WBIR 2006. LNCS, vol. 4057, Springer, Heidelberg (2006)